

Release of NO from Reduced Nitroprusside Ion. Iron-Dinitrosyl Formation and NO-Disproportionation Reactions

Federico Roncaroli,^{†,‡} Rudi van Eldik,^{*,‡} and José A. Olabe^{*,†}

Department of Inorganic, Analytical and Physical Chemistry, INQUIMAE, Faculty of Exact and Natural Sciences, University of Buenos Aires, C1428EHA Buenos Aires, Argentina, and Institute for Inorganic Chemistry, University of Erlangen-Nürnberg, Egerlandstrasse 1, 91058 Erlangen, Germany

Received January 17, 2005

The kinetics and mechanism of the thermal decomposition of the one-electron reduction product of $[\text{Fe}(\text{CN})_5\text{NO}]^{2-}$ (nitroprusside ion, NP) have been studied by using UV–vis, IR, and EPR spectroscopy and mass-spectrometric and electrochemical techniques in the pH range of 4–10. The reduction product contains an equilibrium mixture of $[\text{Fe}(\text{CN})_4\text{NO}]^{2-}$ and $[\text{Fe}(\text{CN})_5\text{NO}]^{3-}$ ions. The first predominates at pH < 8 and is formed by the rapid release of *trans*-cyanide from $[\text{Fe}(\text{CN})_5\text{NO}]^{3-}$, which, in turn, is the main component at pH > 9–10. Both nitrosyl complexes decay by first-order processes with rate constants around 10^{-5} s^{-1} (pH 6–10) related to the dissociation of NO. The decomposition is enhanced at pH 4 by 2 orders of magnitude with protons (and also metal ions) favoring the release of cyanides from the $[\text{Fe}(\text{CN})_4\text{NO}]^{2-}$ ions and the ensuing rapid delivery of NO. At pH 7, an EPR-silent intermediate I_1 is detected (ν_{NO} , 1695 and 1740 cm^{-1}) and assigned to the *trans*- $[\text{Fe}^{\text{II}}(\text{CN})_4(\text{NO})_2]^{2-}$ ion, an $\{\text{Fe}(\text{NO})_2\}^8$ species. At pH 6–8, I_1 induces a disproportionation process with formation of N_2O and the regeneration of nitroprusside in a 1:2 molar ratio. At lower pHs, I_1 leads, competitively, to a second paramagnetic ($S = 1/2$) dinitrosyl intermediate I_2 , $[\text{Fe}(\text{CN})_2(\text{NO})_2]^{1-}$, a new member of a series of four-coordinate $\{\text{Fe}(\text{L})_2(\text{NO})_2\}$ complexes (L = thiolates, imidazole, etc.), described as $\{\text{Fe}(\text{NO})_2\}^9$. Other decomposition products are hexacyanoferrate(II) or free cyanide, depending on the pH, and precipitates of the Prussian-Blue type. This study throws light on the conditions favoring rapid release of NO, to promote vasodilatory effects upon NP injection, and describes new processes related to dinitrosyl formation and NO disproportionation, which are also relevant to the diverse biological processes associated with NO and N_2O processing.

Introduction

Among the metallonitrosyls, sodium pentacyanonitrosylferrate ($\text{Na}_2[\text{Fe}(\text{CN})_5\text{NO}] \cdot 2\text{H}_2\text{O}$, nitroprusside, NP) is widely used in physiological and medical experimentation as a “gold-standard” NO donor drug. NP has a number of clinical uses, the most common of which is hypotensive anaesthesia during surgery.¹ This $\{\text{FeNO}\}^6$ species, in the Enemark–Feltham formalism,² is best described as an Fe(II) center (d^6 , low-spin) containing a NO^+ (nitrosonium) ligand.³ As such, it is extremely inert for thermal dissociation,

although a photoredox process readily delivers NO upon irradiation with UV–vis light.⁴ On the other hand, NP shows electrophilic reactivity toward different nucleophiles (OH^- , amines, thiolates, etc.)^{5,6} and can be reduced chemically or electrochemically forming the paramagnetic one-electron reduction product, $[\text{Fe}^{\text{II}}(\text{CN})_5\text{NO}]^{3-}$, ill-defined two-electron reduction products presumably related to the nitroxyl anion (NO^-), or nitrogen hydrides (NH_2OH , NH_3) through multielectron processes.^{6,7}

* To whom correspondence should be addressed. E-mail: vaneldik@chemie.uni-erlangen.de (R.v.E.); olabe@qi.fcen.uba.ar (J.A.O.).

[†] University of Buenos Aires.

[‡] University of Erlangen-Nürnberg.

- (1) (a) Butler, A. R.; Megson, I. L. *Chem. Rev.* **2002**, *102*, 1155–1165. (b) Wang, P. G.; Xian, M.; Tang, X.; Wu, X.; Wen, Z.; Cai, T.; Janczuk, A. J. *Chem. Rev.* **2002**, *102*, 1091–1134. (c) Clarke, M. J.; Gaul, J. B. *Struct. Bonding (Berlin)* **1993**, *81*, 147–181. (d) Butler, A. R.; Glidewell, C. *Chem. Soc. Rev.* **1987**, *16*, 361–380.

- (2) Enemark, J. H.; Feltham, R. D. *Coord. Chem. Rev.* **1974**, *13*, 339–406. (3) (a) Swinehart, J. H. *Coord. Chem. Rev.* **1967**, *2*, 385–402. (b) Westcott, B. L.; Enemark, J. H. In *Inorganic Electronic Structure and Spectroscopy*; Solomon, E. I., Lever, A. B. P., Eds.; Wiley-Interscience: New York, 1999; Vol. 2, Chapter 7, pp 403–450. (4) Wolfe, S. K.; Swinehart, J. H. *Inorg. Chem.* **1975**, *14*, 1049–1053. (5) Bottomley, F. In *Reactions of Coordinated Ligands*; Braterman, P. S., Ed.; Plenum Press: New York, 1989; Vol. 2, pp 115–222. (6) Olabe, J. A. *Adv. Inorg. Chem.* **2004**, *55*, 61–126. (7) Masek, J.; Maslova, E. *Collect. Czech. Chem. Comm.* **1974**, *39*, 2141–2160.

The vasodilatory action of NP can be observed on the minute time scale after injection. It can be inferred that free NO must be generated in solution in order to activate soluble guanylate cyclase (sGC) to trigger the vasodilation process.¹ Activation involves a very fast (ca. $10^8 \text{ M}^{-1} \text{ s}^{-1}$) coordination of *at least one* NO ligand at the iron center of the enzyme.⁸ The mechanism by which the NO^+ ligand in NP is reduced and released into bodily fluids has not been clearly defined in the literature.^{1,9} It can reasonably be presumed that thiolates or other biologically relevant reductants may be operative at the beginning, but the chemistry of the reduction product(s) is still unclear, particularly those aspects dealing with the rates of dissociation of NO from iron.⁹ It is known that the NO ligand generally promotes ligand labilization at the trans position,^{2,3} and this is the case with reaction 1 for $[\text{Fe}(\text{CN})_5\text{NO}]^{3-}$



The equilibrium in reaction 1 is rapidly established in solution with $k_1 = 2.7 \times 10^2 \text{ s}^{-1}$ and $k_{-1} = 4 \times 10^6 \text{ M}^{-1} \text{ s}^{-1}$ at 25.0 °C.¹⁰ The predominance of $[\text{Fe}(\text{CN})_5\text{NO}]^{3-}$ or $[\text{Fe}(\text{CN})_4\text{NO}]^{2-}$ is strongly pH-dependent, and the relative concentration of the latter species increases with decreasing pH. Both anionic species have been obtained as solid salts and characterized spectroscopically, including structural results for $[\text{Fe}(\text{CN})_4\text{NO}]^{2-}$.^{10,11} Although it has long been recognized that $[\text{Fe}(\text{CN})_5\text{NO}]^{3-}$ is inert for the release of NO,¹² the NO-dissociation rate constant has only recently been measured ($k_{-\text{NO}} = 1.6 \times 10^{-5} \text{ s}^{-1}$, 25.0 °C).¹³ Consequently, the rapid delivery of NO in the biological media has been frequently ascribed to the *labile* $[\text{Fe}(\text{CN})_4\text{NO}]^{2-}$ ion with the additional proposal that the remaining cyanides are subsequently released.¹² No kinetic evidence has been provided for these processes. The timing of the release of

NO vs cyanides from reduced NP is particularly intriguing as is the ensuing fate of NO in the solution. The possibility of further reactivity, other than its eventual coordination to heme proteins (e.g., sGC), should also be considered.

In the studies of coordination of NO to the $[\text{Fe}^{\text{II}}(\text{CN})_5\text{H}_2\text{O}]^{3-}$ ion at pH 7, we found that the initial product $[\text{Fe}(\text{CN})_5\text{NO}]^{3-}$ was unstable under an excess of NO.¹³ A preliminary investigation revealed that $[\text{Fe}(\text{CN})_4\text{NO}]^{2-}$, not $[\text{Fe}(\text{CN})_5\text{NO}]^{3-}$, was the active species promoting decomposition and that NP was formed as one of the products. This result suggested that an NO-disproportionation process could be involved. We, herein, present the results of a stoichiometric and kinetic study in the pH range of 4–10 centered on the spontaneous decay of $[\text{Fe}^{\text{II}}(\text{CN})_5\text{NO}]^{3-}$ and/or $[\text{Fe}(\text{CN})_4\text{NO}]^{2-}$ using UV–vis, IR, EPR, electrochemical, and mass-spectrometric techniques. The study involves avoiding light exposure¹⁴ and maintaining anaerobic conditions. The latter is important because $[\text{Fe}^{\text{II}}(\text{CN})_5\text{NO}]^{3-}$ can be rapidly transformed back to NP in aerobic media.¹⁴ Our studies can be placed in the context of the still underdeveloped chemistry of bound NO in transition metal complexes;¹⁵ we address specifically the nitrosyl transfer problem from a M–NO donor (viz., NP) to another metal acceptor,¹⁶ and we include the possible intermediacy of dinitrosyl compounds.

Experimental Section

General Procedures. All chemicals were of analytical grade and were used without further purification. Eighty-five percent sodium dithionite ($\text{Na}_2\text{S}_2\text{O}_4$) was from Acros. Acetate, bis-tris or phosphate, and borate buffers were used with NaCl to adjust the ionic strength. The pH measurements in the range of 4–10 were done at room temperature with a 744 Metrohm pH meter. The preparation of the solutions was done in Schlenk tubes. The amount of the reducing agent, usually sodium dithionite ($\text{Na}_2\text{S}_2\text{O}_4$) or sodium tetrahydroborate (NaBH_4), necessary for the reaction was added as a solid to N_2 - or Ar-saturated solutions of NP containing the appropriate buffer and ionic strength. At least a 2-fold excess of NP over the reducing agent was always employed. The solutions were always protected from light and were transferred using gastight syringes and a vacuum/Ar or N_2 line. NO was purchased from Air Liquide and purified from higher nitrogen oxides by passing them through an ascarite II column. The concentration of NO in the saturated solutions prepared under NO bubbling was 1.8 mM.

Stoichiometric and Kinetic Results. (a) Chemical Analysis of Reactants and Ionic Products. NP (2–3.5 mg) was dissolved in 10 mL of a 0.01 M buffer solution ($I = 0.1 \text{ M}$, NaCl). $\text{Na}_2\text{S}_2\text{O}_4$ was added, and an aliquot was immediately transferred to a spectrophotometric cell to record the UV–vis spectrum. The initial concentration of the reduced NP species, either $[\text{Fe}(\text{CN})_5\text{NO}]^{3-}$ or $[\text{Fe}(\text{CN})_4\text{NO}]^{2-}$, was calculated considering the molar absorbance values reported in the literature¹⁰ (these values were also checked experimentally in this study). The concentrations usually ranged between 0.2 and 0.5 mM. The samples were allowed to react for 2

- (8) Ballou, D. P.; Zhao, Y.; Brandish, P. E.; Marletta, M. A. *Proc. Natl. Acad. Sci. U.S.A.* **2002**, *99*, 12097–12101.
- (9) Butler, A. R.; Calsy-Harrison, A. M.; Glidewell, C.; Sorensen, P. E. *Polyhedron* **1988**, *7*, 1197–1202.
- (10) Cheney, R. P.; Simic, M. G.; Hoffman, M. Z.; Taub, I. A.; Asmus, K. D. *Inorg. Chem.* **1977**, *16*, 2187–2192.
- (11) (a) Nast, R.; Schmidt, J. *Angew. Chem., Int. Ed. Engl.* **1969**, *8*, 383. (b) van Voorst, J. D. W.; Hemmerich, P. J. *Chem. Phys.* **1966**, *45*, 3914–3918. (c) Schmidt, J.; Kühr, H.; Dorn, W. L.; Kopf, J. *Inorg. Nucl. Chem. Lett.* **1974**, *10*, 55–61. (d) Glidewell, C.; Johnson, I. L. *Inorg. Chim. Acta* **1987**, *132*, 145–147.
- (12) (a) Butler, A. R.; Glidewell, C.; Johnson, I. L.; McIntosh, A. S. *Inorg. Chim. Acta* **1987**, *138*, 159–162. (b) Shafer, P. R.; Wilcox, D. E.; Kruszyna, H.; Kruszyna, R.; Smith, R. P. *Toxicol. Appl. Pharmacol.* **1989**, *99*, 1–10. (c) Wilcox, D. E.; Kruszyna, H.; Kruszyna, R.; Smith, R. P. *Chem. Res. Toxicol.* **1990**, *3*, 71–76. (d) Bates, J. N.; Baker, M. T.; Guerra, R., Jr.; Harrison, D. G. *Biochem. Pharmacol.* **1991**, *42*, S157–S165. (e) Kruszyna, H.; Kruszyna, R.; Rochelle, L. G.; Smith, R. P.; Wilcox, D. E. *Biochem. Pharmacol.* **1993**, *46*, 95–102. (f) Rochelle, L. G.; Kruszyna, H.; Kruszyna, R.; Barchowsky, A.; Wilcox, D. E.; Smith, R. P. *Toxicol. Appl. Pharmacol.* **1994**, *128*, 123–128.
- (13) (a) Roncaroli, F.; Olabe, J. A.; van Eldik, R. *Inorg. Chem.* **2003**, *42*, 4179–4189. (b) Values of NO-dissociation rate constants are very scarce in the literature. By comparison with the dissociation rates of other L ligands in the $[\text{Fe}^{\text{II}}(\text{CN})_5\text{L}]^{3-}$ complexes, NO was shown to be more labile than the strong π -acceptor NO^+ ($k_{-\text{NO}^+}$ cannot be measured from NP) but more inert than NH_3 , a σ -only ligand. We infer that an intermediate σ - π binding of NO to Fe(II), of comparable magnitude to the one for pyrazine or dimethyl sulfoxide, is established.

- (14) Morando, P. J.; Borghi, E. B.; Schteingart, L. M.; Blesa, M. A. *J. Chem. Soc., Dalton Trans.* **1981**, 435–440.
- (15) (a) Ford, P. C.; Lorkovic, I. M. *Chem. Rev.* **2002**, *102*, 993–1018. (b) Ford, P. C.; Laverman, L. E.; Lorkovic, I. M. *Adv. Inorg. Chem.* **2003**, *54*, 203–257.
- (16) Ueno, T.; Suzuki, Y.; Fujii, S.; Vanin, A. F.; Yoshimura, T. *Biochem. Pharmacol.* **2002**, *63*, 485–493.

days in the Schlenk tubes. Then aliquots were extracted, and the different ions present in the final solutions were analyzed using spectrophotometric techniques. The latter procedures were not performed under anaerobic conditions. A Hewlett-Packard 8453A diode array spectrophotometer was employed for the UV–vis measurements. The *o*-phenanthroline and SCN^- reagents were used to determine the concentrations of $[\text{Fe}(\text{H}_2\text{O})_6]^{2+}$ and $[\text{Fe}(\text{H}_2\text{O})_6]^{3+}$, respectively.¹⁷ Nitrite was quantified using the *Griess* reaction.¹⁸ Free CN^- or HCN was determined with an Aquaquant 14429 kit from Merck. NP was determined through the reaction with thiosuccinic acid,¹⁹ as described elsewhere.²⁰ The final value was corrected using the initial concentration of NP. By knowing the amount that was reduced from the initial spectrum, we determined the concentration of NP that was effectively obtained through the reoxidation of $[\text{Fe}(\text{CN})_5\text{NO}]^{3-}$. The concentration of $[\text{Fe}(\text{CN})_6]^{4-}$ was determined from the reaction with $[\text{Fe}(\text{H}_2\text{O})_6]^{3+}$ producing Prussian-Blue.²¹ The sample was mixed with an equal volume of a 0.1 M HNO_3 solution containing 1 mM $\text{Fe}(\text{NO}_3)_3$. Calibration was achieved by preparing standard solutions of $[\text{Fe}(\text{CN})_6]^{4-}$ in the range of 0–0.2 mM. Samples and standard solutions were allowed to react for 2 h, and the absorbance at 705 nm was measured. No precipitation of Prussian-Blue was observed under these conditions, and the calibration curve showed a good linear distribution.

(b) UV–Vis Spectroscopy. (i) Slow Processes. Samples (ca. 0.2 mM in the reduced species, 0.01 M in buffer, and $I = 0.1$ M) were transferred to a cell with a 1 cm optical path, under N_2 . The absorbance changes in the range of 300–800 nm were recorded on a double-beam Varian Cary 5G spectrophotometer equipped with a temperature control system. The results were analyzed with the SPECFIT program²² using a two-exponential model ($A \rightarrow B \rightarrow C$) for the reaction at pH 4–8 and a single-exponential model ($A \rightarrow B$) for the one at pH 9–10. The molar absorbance values of the intermediates were estimated by calculating the initial complex concentration through the molar absorbance reported in the literature.¹⁰ Analyses of residuals from the SPECFIT treatments are presented in Figure S11. All of the reactions were done at 25.5 ± 0.2 °C.

(ii) Stopped-Flow (SF) Measurements. NO-saturated solutions were prepared as described elsewhere.²⁰ The ionic strength was 0.1 M (NaCl), and the buffer concentration was 0.01 M (pH 5–7). NP was reduced with $\text{Na}_2\text{S}_2\text{O}_4$ in the buffer solutions, and the final reduced complex was 10-fold substoichiometric with respect to NO. The NO and complex solutions were mixed with a SX 18MV Applied Photophysics SF instrument at 25.0 ± 0.1 °C. Kinetic traces were recorded at 620, 420, and 330 nm and were fitted to a single exponential over more than 3 half-lives. The observed rate constants did not differ significantly at the different wavelengths.

(c) IR Spectroscopy. NP (100 mg) was dissolved in 10 mL of a solution 0.5 M in buffer (without the addition of NaCl) in H_2O or D_2O , depending on the spectral range under study. $\text{Na}_2\text{S}_2\text{O}_4$

(30 mg) was added after saturation with Ar, and then the solution was immediately transferred to the IR liquid cell. The rest of the solution was stored in a syringe which was kept in a large Schlenk tube under Ar to prevent any reaction with air. From time to time, aliquots of the solution were loaded in the cell and the IR spectrum was recorded with a Thermo Nicolet Avatar 320 FT-IR spectrometer and a Spectratech liquid cell containing two 32×3 mm CaF_2 disks and a 0.1 mm spacer. The spectral ranges were 1750–2800 and 2150–1300 cm^{-1} in the H_2O and D_2O solutions, respectively. The reaction of NO with the $[\text{Fe}(\text{CN})_4\text{NO}]^{2-}$ complex was studied by bubbling NO through the complex solution.

To perform the labeling experiments starting with $[\text{Fe}(\text{CN})_5^{15}\text{NO}]^{2-}$, we added 55 mg of $\text{Na}_3[\text{Fe}(\text{CN})_5\text{NH}_3] \cdot 3\text{H}_2\text{O}$ ²³ to a deoxygenated solution of 12 mg of $\text{Na}^{15}\text{NO}_2$ (Aldrich) in 20 mL of H_2O . The solution was allowed to react for 1 h, and then HCl was added to reach pH 2–4. Four hours later, the solution was evaporated to dryness. The residue was dissolved in a few milliliters of D_2O and evaporated again. The IR spectrum was checked for comparison with reported values for NP labeled with ^{15}NO .²⁴ For the labeling experiments, this sample was dissolved in 5 mL of D_2O together with the buffer system (pH 7). Finally, $\text{Na}_2\text{S}_2\text{O}_4$ was added as described for the other IR experiments.

(d) EPR Spectroscopy. Samples (0.3 mM in the reduced species, 0.01 M in buffer, and $I = 0.1$ M) were prepared as described before and kept at 25.5 °C during the experiment. From time to time, aliquots were extracted and transferred under N_2 to EPR quartz tubes. Each sample was frozen immediately in liquid N_2 . After all of the samples were collected, they were measured in the X-band of a Bruker ESP 300E spectrometer. The spectra were recorded at 9.44 GHz, 0.635 mW power, 100 kHz modulation frequency, and 9.3434 G modulation amplitude. To study the reaction between NO and the $[\text{Fe}(\text{CN})_4\text{NO}]^{2-}$ complex, we prepared the solutions as already described and bubbled NO through them. They were, then, transferred to the EPR tube and frozen. The *g* values were estimated by using the magnetic field and the microwave frequency without performing a calibration.

(e) Electrochemical Detection of NO. An amiNO electrode from Innovative Instruments, Inc., was used. The electrode was attached to a homemade potentiostat interfaced to a computer. For these measurements, 10 mg of NP was dissolved in 10 mL of Ar-saturated 0.1 M buffer solutions. After allowing for equilibration of the electrode output, we added 3 mg of $\text{Na}_2\text{S}_2\text{O}_4$ and recorded the current as a function of time. FeSO_4 , CuSO_4 , CoSO_4 , MnSO_4 , and NiCl_2 (9–10 mM at pH 7.0) were used to study the influence of metal ions. KSCN (20 mM), *o*-phenanthroline, or disodium ethylenediaminetetraacetate was used to study the influence of other ligands.

(f) Mass-Spectrometric Determinations of N_2O . A 0.5 M buffered solution containing 100 mg of NP in 10 mL was transferred to a mechanically stirred reactor (volume ca. 24 mL) attached to a vacuum system. After evacuation, 30 mg of $\text{Na}_2\text{S}_2\text{O}_4$ was added from a side flask. The reactor was linked through a capillary to a SenSym SX15A pressure sensor and to an Extrel Emba II mass spectrometer. The temperature was controlled at 25 °C. The evolution of the total pressure as a function of time was recorded during the experiment. At the end, the composition of the gaseous products was analyzed with the mass spectrometer.²⁵

(17) Vogel, A. *A Textbook of Quantitative Inorganic Analysis Including Elementary Instrumental Analysis*, 4th ed.; Longman Inc.: New York, 1978.

(18) Schmidt, H. H. H. W.; Kelm, M. In *Methods in Nitric Oxide Research*; Feilisch, M.; Stamler, J. S., Eds.; Wiley: Chichester, UK, 1996; Part VII, Chapter 33.

(19) Szacilowski, K.; Stochel, G.; Stasicka, Z.; Kisch, H. *New J. Chem.* **1997**, 21, 893–902.

(20) Roncaroli, F.; Olabe, J. A.; van Eldik, R. *Inorg. Chem.* **2002**, 41, 5417–5425.

(21) Sharpe, A. G. *The Chemistry of Cyano Complexes of the Transition Metals*; Academic Press: London, 1976.

(22) Binstead, R. A.; Zuberbulher, A. D. *SPECFIT*; Spectrum Software Associates: Chapel Hill, NC, 1993–1999.

(23) Kenney, D. J.; Flynn, T. P.; Gallini, J. B. *J. Inorg. Nucl. Chem.* **1961**, 20, 75.

(24) Chacón Villalba, M. E.; Varetto, E. L.; Aymonino, P. J. *Vib. Spectrosc.* **1997**, 14, 275–286.

(25) Gutiérrez, M. M.; Amorebieta, V. T.; Estiú, G. L.; Olabe, J. A. *J. Am. Chem. Soc.* **2002**, 124, 10307–10319.

Table 1. IR and UV–Vis Spectroscopic Data for Reactants, Intermediates, and Products

compound	stretching frequencies (cm ⁻¹)	λ_{\max} (nm) (ϵ , M ⁻¹ cm ⁻¹)
[Fe(CN) ₅ NO] ²⁻	2142, 1936 ²⁶	498 (8), 394 (25), 330 (40) ²⁷
[Fe(CN) ₄ NO] ²⁻	2115, 1800 ²⁶	615 (380), 430 (100), 350 (300) ¹⁰
[Fe(CN) ₅ NO] ³⁻	2088, 1648 ²⁶	430 (550), 345 (3500) ¹⁰
[Fe(CN) ₆] ⁴⁻	2038 ²⁶	422 (5), 322 (300) ²⁸
[Fe(CN) ₄ (OH)NO] ²⁻	1910 ¹⁰	
[Fe(CN) ₄ (NO) ₂] ²⁻ (I ₁)	1695, 1737	333 (600), 425 (200), 600 (120)
[Fe(CN) ₂ (NO) ₂] ⁻ (I ₂)	1810, 1737	330 (650), 400 (300), 500 (150)
N ₂ O	2230 ²⁹	

Results

A summary of the compounds that appear as main reactants, products, or proposed reaction intermediates along with the relevant IR and UV–vis spectroscopic data is presented in Table 1.^{10,26–28}

(a) pH 9–10. Predominance of [Fe(CN)₅NO]³⁻ at the Beginning of Decomposition. The [Fe(CN)₅NO]³⁻ ion is the most predominant initial species in this pH range after the fast reduction of NP and the establishment of equilibrium 1. Figure 1 shows the successive UV–vis spectra revealing a decreasing intensity of the absorption bands of [Fe(CN)₅NO]³⁻ (Table 1). The single-exponential decay is valid over 3 half-lives affording a value of $k_{\text{obs}} = 4 \times 10^{-5} \text{ s}^{-1}$ at pH 9. Note that some [Fe(CN)₄NO]²⁻ can be observed through the weak absorption at ca. 620 nm.

Figure 2 shows the successive spectra for the IR measurements in D₂O. An intensity decrease can be observed for the stretching vibrations of the cyano and NO groups in [Fe(CN)₅NO]³⁻ at 2088 and 1648 cm⁻¹, respectively.²⁶ Product formation is associated with the onset of a new band at 2038 cm⁻¹, typical of the [Fe(CN)₆]⁴⁻ ion.^{21,26} The concentration of this ion was also determined in the solutions (ca. 20–30% with respect to initially reduced species), although a strictly quantitative evaluation was disturbed by the formation of precipitates. Again, minor quantities of [Fe(CN)₄NO]²⁻ were detected through the bands at 2115 and 1800 cm⁻¹.²⁶ A weak shoulder at 1910 cm⁻¹ can be assigned to [Fe(CN)₄(OH)(NO)]²⁻.¹⁰ NO was detected electrochemically during the first 15 min and was absent after 10 h. N₂O was also observed in the IR spectra (not shown) after ca. 10 h of reaction through its characteristic band at 2230 cm⁻¹.²⁹ Nitrite was also detected over the whole pH range of 4–10 (yield < 5%). Finally, Figure 2 allows us to detect some gradual increase in the characteristic absorptions of NP at 2142 and 1936 cm⁻¹.²⁶ The quantitative determination at the end of reaction showed, at pH 10, around a 10% yield of NP with respect to the initial [Fe(CN)₅NO]³⁻ concentration.

(b) pH 6–8. Decomposition of Mixtures of [Fe(CN)₅NO]³⁻ and [Fe(CN)₄NO]²⁻. Figure 3a shows the

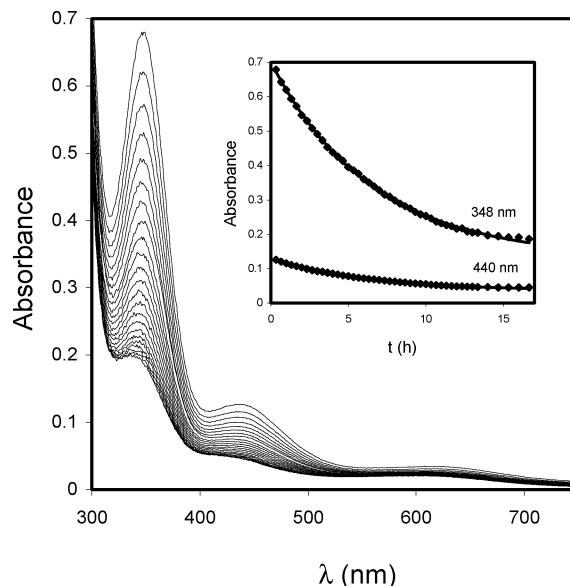


Figure 1. UV–vis spectral changes observed during the decomposition of a ca. 0.2 mM reduced nitroprusside solution (reductant: Na₂S₂O₄) at pH 9.0 ($I = 0.1 \text{ M}$, $T = 25.5 \text{ }^\circ\text{C}$, 0.01 M borate buffer) with a cycle time of 2400 s. Inset: kinetic traces at 348 and 440 nm fitted to a single exponential by SPECFIT, $k_{\text{obs}} = (4.0 \pm 0.3) \times 10^{-5} \text{ s}^{-1}$.

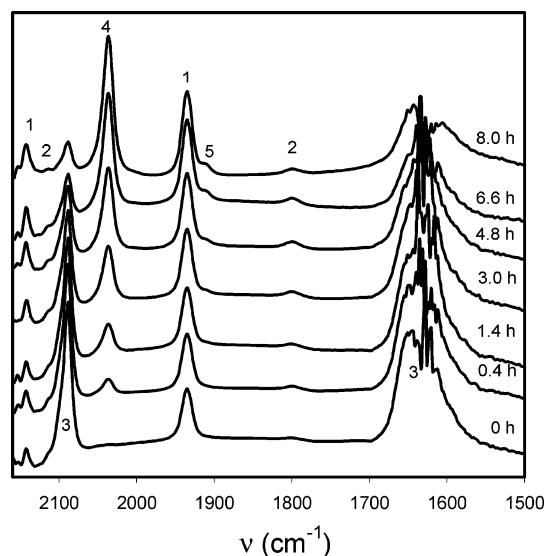


Figure 2. IR spectral changes recorded during the decomposition of a solution ca. 17 mM in reduced nitroprusside (reductant: Na₂S₂O₄) at pH 10 ($T = 25 \text{ }^\circ\text{C}$, 0.5 M borate buffer) in D₂O: $k_{\text{obs}} \approx 4 \times 10^{-5} \text{ s}^{-1}$ (decay of ν_{NO}). Peak numbers correspond to the following (as detailed in Table 1): 1, [Fe(CN)₅NO]²⁻; 2, [Fe(CN)₄NO]²⁻; 3, [Fe(CN)₅NO]³⁻; 4, [Fe(CN)₆]⁴⁻; and 5, [Fe(CN)₄(OH)NO]²⁻.

successive UV–vis spectra with significant quantities of both complexes at the beginning. The inset includes the absorbance traces at two selected wavelengths fitted to a two-exponential model. A monotonic decay at 615 nm along with an initial increase and subsequent decrease of an intermediate I₁ with maximum at 336 nm can be observed. The output leads to values of $k_{\text{first}} = 3\text{--}6 \times 10^{-5} \text{ s}^{-1}$ for the first reaction step and of $k_{\text{second}} = 1\text{--}2 \times 10^{-5} \text{ s}^{-1}$ for the second one, involving the formation and decay of the intermediate I₁, respectively. Figure 3b shows the Specfit spectra calculated for the reactant, the intermediate, and the product. Table 1 includes the calculated absorbance maxima for I₁. Similar

(26) Schwane, J. D.; Ashby, M. T. *J. Am. Chem. Soc.* **2002**, *124*, 6822–6823.

(27) Manoharan, P. T.; Gray, H. B. *Inorg. Chem.* **1966**, *5*, 823–839.

(28) Gray, H. B.; Beach, N. A. *J. Am. Chem. Soc.* **1963**, *85*, 2922–2926.

(29) Sampath, V.; Rousseau, D. L.; Caughey, W. S. In *Methods in Nitric Oxide Research*; Feilisch, M., Stamler, J. S., Eds.; Wiley: Chichester, U.K., 1996; Part VI, Chapter 29.

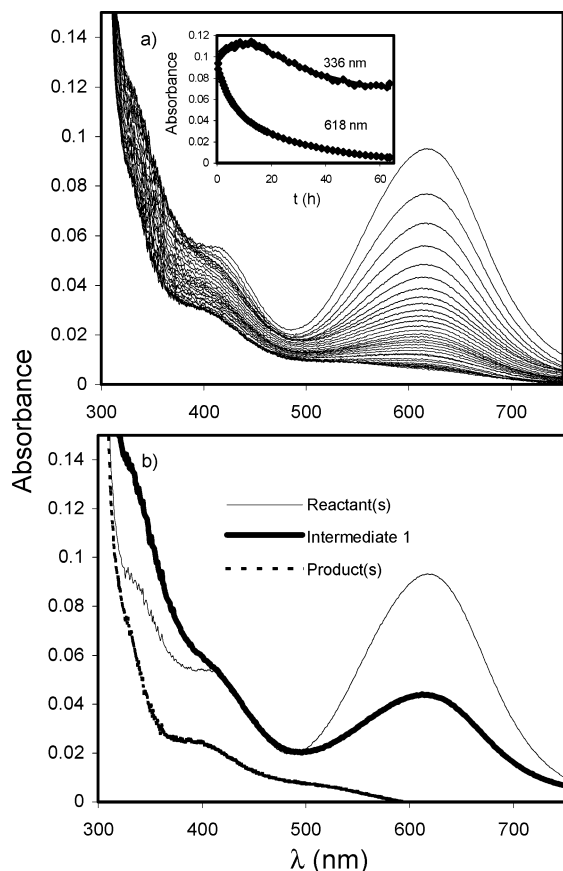


Figure 3. (a) UV-vis spectral changes observed during the decomposition of a solution ca. 0.25 mM in reduced NP (reductant: $\text{Na}_2\text{S}_2\text{O}_4$) at pH 6.0 ($I = 0.1$ M, $T = 25.5$ °C, 0.01 M bis-tris buffer) with a cycle time of 7200 s. Inset: kinetic traces at 336 and 618 nm fitted to a double-exponential model by SPECFIT, $k_{\text{first}} = (5.4 \pm 0.2) \times 10^{-5} \text{ s}^{-1}$, $k_{\text{second}} = (9.3 \pm 0.5) \times 10^{-6} \text{ s}^{-1}$. (b) Spectra of the reactants, intermediates, and products obtained from the SPECFIT analysis.

Table 2. UV-Vis Kinetic Data Obtained for the Spontaneous Decomposition of the Mixture of $[\text{Fe}(\text{CN})_5\text{NO}]^{3-}$ and $[\text{Fe}(\text{CN})_4\text{NO}]^{2-}$ as a Function of pH^a

pH	$k_{\text{first}} (\times 10^5 \text{ s}^{-1})$	$k_{\text{second}} (\times 10^5 \text{ s}^{-1})$
10.0	2.5 ± 0.5	—
9.0	3.5 ± 0.5	—
8.0	5.3 ± 0.5	1.5 ± 0.5
7.0	2.7 ± 0.2	1.1 ± 0.5
6.0	5.5 ± 0.1	0.9 ± 0.3
5.0	20 ± 0.5	1.4 ± 0.3
4.0	200 ± 0.5	not measured

^a Reported values correspond to average values of at least two independent measurements. Errors were estimated from the difference between those values. $T = 25.5$ °C, 0.01 M buffer, $I = 0.1$ M (NaCl). See text for the determination of rate constants.

spectral and kinetic data were obtained by using either dithionite or tetrahydroborate as reducing agents. Table 2 reports the kinetic results in all of the studied pH ranges.

The chronoamperograms recorded in Figure 4 show that NO is generated rapidly during the first minutes with the rate increasing as the pH decreases. The concentration of NO remains constant or decreases with time. For N_2O , the mass-spectrometric measurements reveal a continuous exponential increase in the pressure in the reactor with $k_{\text{obs}} = 1.4 \times 10^{-5} \text{ s}^{-1}$ for the formation rate.

At the end of the reaction, $[\text{Fe}(\text{CN})_6]^{4-}$ was found in low yields, in contrast with free cyanides (60–200% with re-

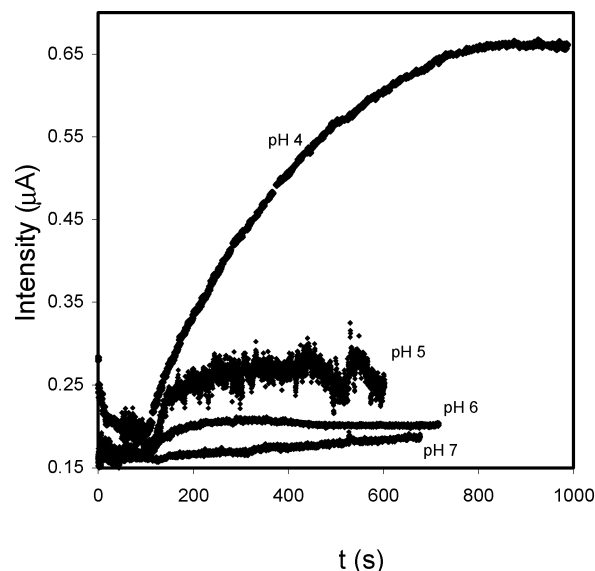


Figure 4. Chronoamperograms for the release of NO after addition of 3 mg of $\text{Na}_2\text{S}_2\text{O}_4$ to 10 mL of a 3.4 mM nitroprusside solution at different pHs.

spect to initial reduced complex), together with some ferrous and ferric ions and a white precipitate, presumably $\text{Fe}_2[\text{Fe}(\text{CN})_6]$.²¹ The relative yields of NP and N_2O were 40% and 20%, respectively, with respect to initial reduced NP concentration.

The successive IR spectra in Figure 5a (pH 7, D_2O solution) show a decrease in the intensity of the bands for both the $[\text{Fe}(\text{CN})_5\text{NO}]^{3-}$ and $[\text{Fe}(\text{CN})_4\text{NO}]^{2-}$ ions along with an absorption increase at 2038 cm^{-1} ($[\text{Fe}(\text{CN})_6]^{4-}$ and/or other Fe-cyano-aqua complexes). The absorption increase at 2142 and 1936 cm^{-1} corresponding to NP is again clearly observed, and the peak at 2230 cm^{-1} for N_2O is apparent at ca. 3–6 h after the start of decomposition (cf. Figure S12, measurements in H_2O). Another outstanding feature is given by the appearance of a weak absorption at 1695 cm^{-1} (with a maximum intensity attained around 2.5 h) which is absent at the beginning and end of the process revealing its intermediate character (we assign these IR features to I_1 ; see Discussion). Finally, Figure 5b again shows the peak at 1695 cm^{-1} and a weaker absorption at ca. 1737 cm^{-1} after a complementary experiment with a controlled addition of NO to $[\text{Fe}(\text{CN})_4\text{NO}]^{2-}$ was performed. These peaks disappear under a further excess of NO.

In the IR labeling experiments with $[\text{Fe}(\text{CN})_4^{15}\text{NO}]^{2-}$, Figure S13 shows that the intermediate I_1 appears ca. 2 h after the beginning of the spontaneous decomposition. As expected, it shows that all of the relevant peaks associated with ν_{NO} stretchings (Table 1) are shifted downward by ca. 40 cm^{-1} , including the band previously assigned to the I_1 complex at 1695 cm^{-1} which now develops at 1655 cm^{-1} . In a second complementary experiment with unlabeled NO bubbling through a fresh solution of $[\text{Fe}(\text{CN})_4^{15}\text{NO}]^{2-}$, Figure S14 shows that a shoulder assignable to I_1 appears at ca. 1670 cm^{-1} . Interestingly, two absorptions for the emerging NP complex can be observed. In addition to the one at 1897 cm^{-1} , corresponding to $[\text{Fe}(\text{CN})_5^{15}\text{NO}]^{2-}$,²⁴ another one shows up at 1936 cm^{-1} , corresponding to $[\text{Fe}(\text{CN})_5^{14}\text{NO}]^{2-}$.

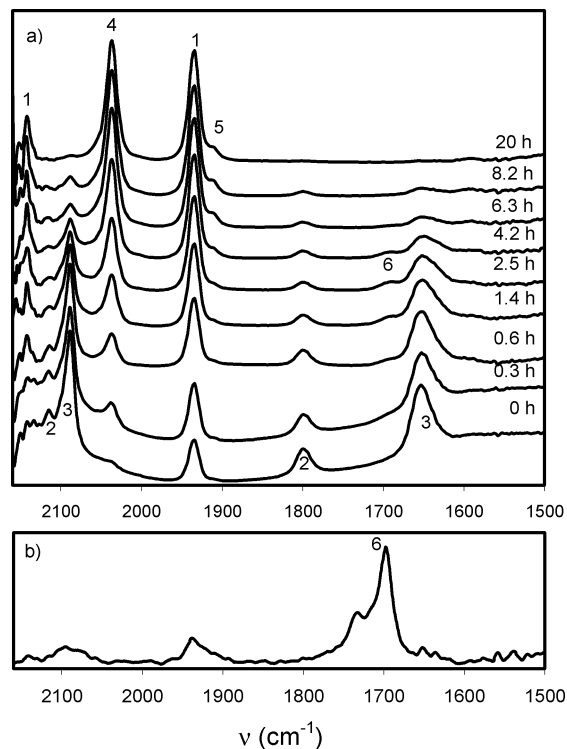


Figure 5. (a) IR spectral changes observed during the decomposition of a solution ca. 17 mM in reduced NP (reductant: $\text{Na}_2\text{S}_2\text{O}_4$) at pH 7 ($T = 25^\circ\text{C}$, 0.5 M phosphate buffer) in D_2O , $k_{\text{obs}} \approx 5 \times 10^{-5} \text{ s}^{-1}$ (decay of ν_{NO}). (b) Spectrum obtained after bubbling NO through a reduced nitroprusside solution until first color change (17 mM in D_2O). A detailed description of the spectral changes is given in the text. Peak numbers correspond to the following (as detailed in Table 1): 1, $[\text{Fe}(\text{CN})_5\text{NO}]^{2-}$; 2, $[\text{Fe}(\text{CN})_4\text{NO}]^{2-}$; 3, $[\text{Fe}(\text{CN})_5\text{NO}]^{3-}$; 4, $[\text{Fe}(\text{CN})_6]^{4-}$; 5, $[\text{Fe}(\text{CN})_4(\text{OH})\text{NO}]^{2-}$; and 6, $[\text{Fe}(\text{CN})_4(\text{NO})_2]^{2-}$.

In the EPR measurements (not shown), the intensity of the reactant's signal decreases exponentially, with a rate constant of ca. $5 \times 10^{-5} \text{ s}^{-1}$, affording an EPR-silent product. Values on the same order of magnitude ($k = \text{ca. } 5\text{--}8 \times 10^{-5} \text{ s}^{-1}$) may be estimated from the IR data in Figure 5a by measuring the intensity decrease of ν_{NO} .

(c) pH 4–5. Fast Decomposition of Predominant $[\text{Fe}(\text{CN})_4\text{NO}]^{2-}$. The UV–vis spectral runs reveal a significant increase in the decomposition rate for the $[\text{Fe}(\text{CN})_4\text{NO}]^{2-}$ ion, as detailed in Table 2. This is confirmed by the electrochemical experiments on release of NO. Figure 4 shows a consistent increase in the rate and amount of NO produced at pH 4 within the first minutes. From the exponential display, we estimate a value for k_{NO} , in fair agreement with the kinetic data in Table 2, of ca. $2 \times 10^{-3} \text{ s}^{-1}$.

Although our experimental setup had a headspace, we believe that this does not alter our conclusions. Since all of the experiments were done under the same conditions, we believe that a comparison between the results at different pH levels can still be made. At pH 4, the value of k_{NO} (ca. $2 \times 10^{-3} \text{ s}^{-1}$) could be affected to some degree by the loss of NO on the minute time scale. However, the order of magnitude of k_{NO} is in good agreement with that measured spectrophotometrically.

NP is also formed in a 50% yield at the end of reaction along with high yields of cyanide (300%), aqueous Fe(III),

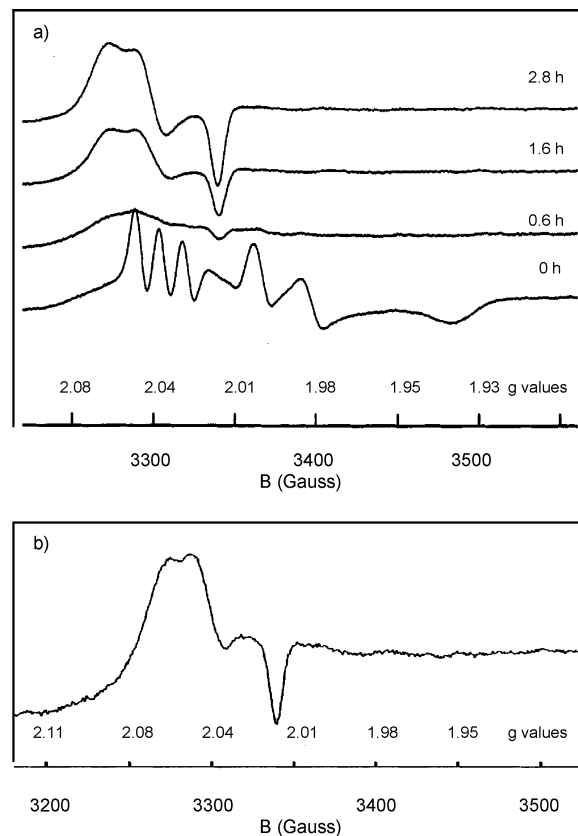


Figure 6. (a) EPR spectral changes recorded during the decomposition of a solution ca. 0.26 mM in reduced nitroprusside (reductant: NaBH_4) at pH 5.0 ($I = 0.1 \text{ M}$, $T = 25^\circ\text{C}$, 0.01 M acetate buffer). (b) Spectrum obtained after bubbling NO through a reduced nitroprusside solution (0.26 mM, $I = 0.1 \text{ M}$, 0.01 M acetate buffer).

and Prussian-Blue type precipitates. N_2O is also observed in the IR spectra (Figure S15).

Figure 6a shows the successive EPR spectra obtained at pH 5. The signals of the reactant decay³⁰ evolve through an apparently silent intermediate (second spectrum from bottom) to reach a final different spectrum (which also decays for longer times). The last spectrum is similar to those reported in the literature for the four-coordinate $\{\text{Fe}(\text{L})_2(\text{NO})_2\}$ compounds ($S = 1/2$, $\text{L} = \text{thiolates, imidazole, CO, etc.}$) called “ $g = 2.03$ ” dinitrosyl iron complexes (DNIC).³¹ It is also similar to the one obtained after bubbling NO through the reduced NP solution (Figure 6b), and we identify it as I_2 .

(30) The initial EPR spectrum in Figure 6a shows the presence of both the tetracyanonitrosyl and pentacyanonitrosyl species. The percentage of each species is strongly affected by the temperature. Only the tetracyanonitrosyl ion gives an EPR signal at 22°C .^{12d} The final spectrum in Figure 6a and the one in Figure 6b agree with those reported for the four-coordinated dinitrosyls.³¹

(31) (a) Lee, M.; Arosio, P.; Cozzi, A.; Chasteen, N. D. *Biochemistry* **1994**, *33*, 3679–3687. (b) Vanin, A. F.; Serezhnikov, V. A.; Mikoyan, V. D.; Genkin, M. V. *Nitric Oxide* **1998**, *2*, 224–234. (c) Reginato, N.; McCrory, C. T. C.; Pervitsky, D.; Li, L. *J. Am. Chem. Soc.* **1999**, *121*, 10217–10218. (d) Butler, A. R.; Glidewell, C.; Hyde, A. R.; Walton, J. C. *Polyhedron* **1985**, *4*, 797–809. (e) Costanzo, S.; Menage, S.; Purrello, R.; Bonomo, R.; Fontecave, M. *Inorg. Chim. Acta* **2001**, *318*, 1–7. (f) Burlamaschi, L.; Martín, G.; Tiezzi, E. *Inorg. Chem.* **1969**, *8*, 2021–2025. (g) McDonald, C. C.; Phillips, W. D.; Mower, H. F. *J. Am. Chem. Soc.* **1965**, *87*, 3319–3326. (h) Ueno, T.; Yoshimura, T. *Jpn. J. Pharmacol.* **2000**, *82*, 95–101. (i) Foster, M. W.; Cowan, J. A. *J. Am. Chem. Soc.* **1999**, *121*, 4093–4100. (j) Bryar, T. R.; Eaton, D. R. *Can. J. Chem.* **1992**, *70*, 1917–1926.

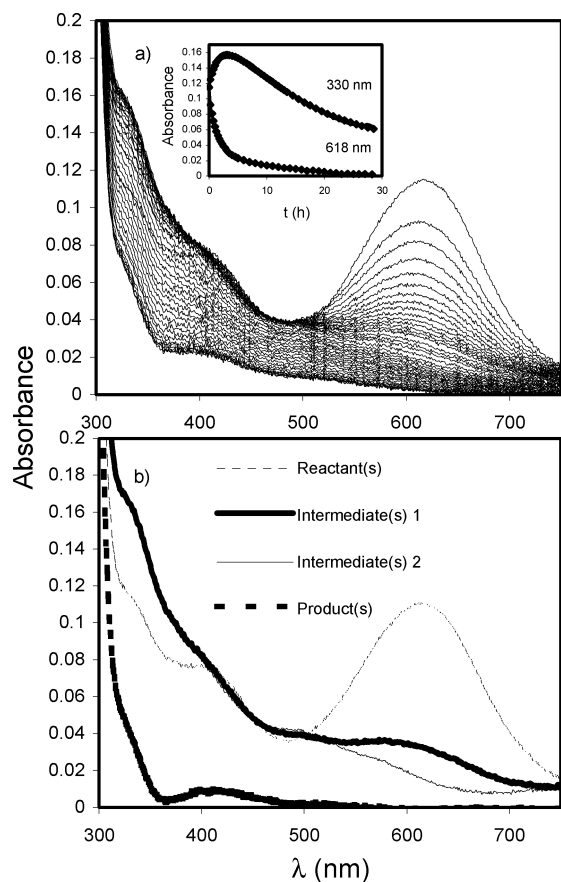


Figure 7. (a) UV-vis spectral changes recorded during the decomposition of a solution ca. 0.32 mM in reduced nitroprusside (reductant: NaBH_4) at pH 5.0 ($I = 0.1 \text{ M}$, $T = 25.5 \text{ }^\circ\text{C}$, 0.01 M acetate buffer) with cycle times of 900 and 3600 s after 18000 s. Inset: kinetic traces at 330 and 618 nm fitted to a three-exponential model by SPECFIT, $k_{\text{first}} = (2.4 \pm 0.2) \times 10^{-4} \text{ s}^{-1}$, $k_{\text{second}} = (5.1 \pm 0.5) \times 10^{-5} \text{ s}^{-1}$, and $k_{\text{third}} = (2.4 \pm 0.7) \times 10^{-5} \text{ s}^{-1}$. (b) Spectra of the reactants, intermediates, and products obtained from the SPECFIT analysis.

In Figure 7, both dinitrosyl intermediates, I_1 and I_2 , can be detected in the UV-vis spectra when tetrahydroborate is used following a SPECFIT analysis with a three exponential model. Only I_2 is observed when dithionite is used (Figure SI 6). Table 1 shows the calculated UV-vis absorption parameters for I_2 .

Figure 8a shows the IR spectra obtained in the D_2O solution at pH 4. The decay of the bands from $[\text{Fe}(\text{CN})_4\text{NO}]^{2-}$ can be observed, and the product formation is associated with increasing absorptions apparently corresponding to the following three processes: (i) formation of NP consistent with bands at 1936 and 2142 cm^{-1} and with the chemical analysis at the end of reaction, (ii) Fe(II) and Fe(III) Prussian-Blue type species corresponding to a broad envelope in the 2000–2080 cm^{-1} region,²¹ and (iii) an increase and further decrease of a new absorption at 1737 cm^{-1} , assigned to I_2 . This process correlates with the shift of the band from 1800 to 1810 cm^{-1} . The absorptions of the I_2 intermediate at 1810 and 1737 cm^{-1} can also be observed in Figure 8b after bubbling NO through a solution of the reactant.

An interesting feature in the experiments at pH 4–5 was related to the influence of the addition of cyanide. This led to a behavior similar to that reported above for higher pHs;

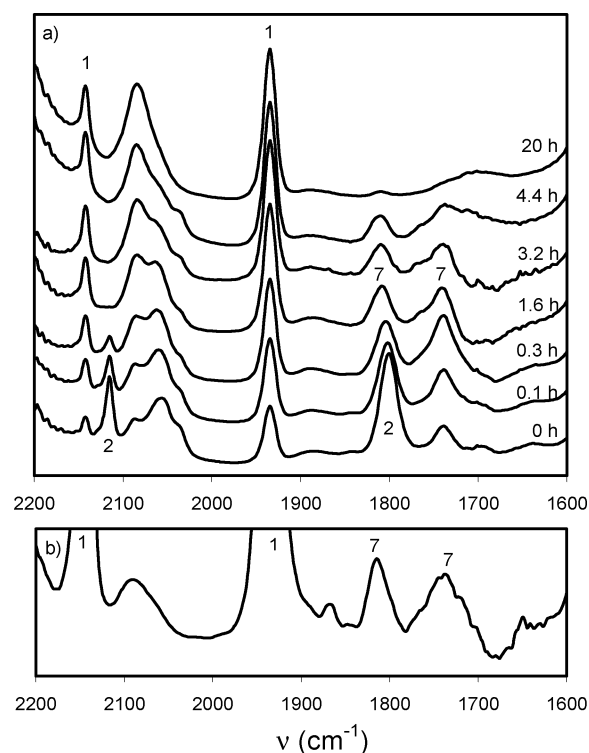


Figure 8. (a) IR spectral changes observed during the decomposition of a solution ca. 17 mM in reduced nitroprusside (reductant: $\text{Na}_2\text{S}_2\text{O}_4$) at pH 4 ($T = 25 \text{ }^\circ\text{C}$, 0.5 M acetate buffer) in D_2O , $k_{\text{obs}} \approx 1 \times 10^{-3} \text{ s}^{-1}$ (decay of ν_{NO}). (b) Spectrum obtained after bubbling NO through a reduced nitroprusside solution (17 mM, 0.5 M acetate buffer) in D_2O . A detailed description of the spectral changes is given in the text. Peak numbers correspond to the following (as detailed in Table 1): 1, $[\text{Fe}(\text{CN})_5\text{NO}]^{2-}$; 2, $[\text{Fe}(\text{CN})_4\text{NO}]^{2-}$; and 7, $[\text{Fe}(\text{CN})_2(\text{NO})_2]^-$. The broad envelope at 2000–2100 cm^{-1} corresponds to a mixture of soluble and/or colloidal Fe(II)–cyano or Fe(II)–cyano–aqua complexes.

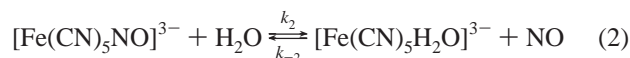
i.e., lower decomposition rates were observed, and the I_1 intermediate could be detected again in the experiment with dithionite.

(d) Influence of Added Metal Ions. Figure SI7 shows the influence of different metal ions on the rate of release of NO. A rapid increase ($\text{Cu} > \text{Co} > \text{Fe}$) is observed for the short times after addition followed by a slower increase for the last two ions and a distinctive decrease for copper. The influence of metal ions probably occurs because of association effects on bound cyanides, promoting the decomposition of $[\text{Fe}(\text{CN})_4\text{NO}]^{2-}$. It is also related to the ability to form stable complexes with cyanide. This is equivalent to the pH effect noted above. The presence of metal ions is highly feasible in biological media, thus allowing for a fast decomposition process even at pH conditions around 7 which are insufficiently low to promote the complete release of cyanide. We also checked the influence of added ligands on the release of NO. We found that thiocyanate, *o*-phenanthroline, and EDTA enhanced the decomposition rate of the complex (viz., cyanide release), but surprisingly, no effect on the release of NO was observed.

Discussion

The observed rate constant for the decay of reduced NP at pH 10 is 2–3 times larger than the value previously

measured for $[\text{Fe}(\text{CN})_5\text{NO}]^{3-}$, reaction 2 ($k_2 = k_{-\text{NO}}$)^{13,32}

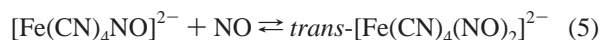
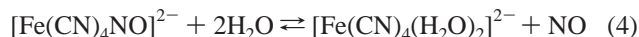


The difference arises from the fact that, under our reaction conditions, a small amount of $[\text{Fe}(\text{CN})_4\text{NO}]^{2-}$ is present in the equilibrium mixtures described by reaction 1 (cf. UV-vis and IR spectra). The formation of hexacyanoferrate(II) observed occurs through a follow-up to reaction 2, viz. the thermal decomposition of $[\text{Fe}(\text{CN})_5\text{H}_2\text{O}]^{3-}$, which evolves according to the stoichiometry in eq 3



Reaction 3 has previously been analyzed mechanistically on the basis of a set of competitive-consecutive reactions.³³ The rate-determining first-order decay of $[\text{Fe}(\text{CN})_5\text{H}_2\text{O}]^{3-}$ leads to $[\text{Fe}(\text{CN})_4(\text{H}_2\text{O})_2]^{2-}$ with $k_{-\text{CN}} = 1.25 \times 10^{-4} \text{ s}^{-1}$ (25.0 °C, $I = 1 \text{ M}$). The successive release of the remaining cyanides is faster as is the reverse coordination of CN^- to the reacting $[\text{Fe}(\text{CN})_5\text{H}_2\text{O}]^{3-}$ ion.³³ The products in reaction 3 lead to the formation of Prussian-Blue type precipitates, as observed in some of our experiments, unless the solutions are sufficiently dilute.^{21,33}

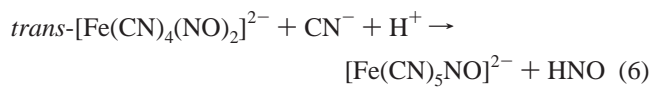
The results at pH 10 show the formation of NP and N_2O as additional products, although in minor amounts when compared to those obtained at pH 6–7. In this pH range, the UV-vis, IR, and EPR spectra reveal the distinctive formation of intermediate I_1 . We propose it to be a *trans*-dinitrosyl species which forms after the dissociation of NO from the $[\text{Fe}(\text{CN})_4\text{NO}]^{2-}$ ion, eq 4, and the subsequent coordination to the same complex, eq 5



The EPR-silent properties of I_1 can be ascribed to a low-spin Fe(II) center containing two antiferromagnetically coupled NO ligands. Support for the product identification in eq 5 is provided by kinetic evidence: the SF experiment in which excess NO reacts with $[\text{Fe}(\text{CN})_4\text{NO}]^{2-}$ shows a first-order rate law in each reactant with $k_5 = 4.3 \times 10^4 \text{ M}^{-1} \text{ s}^{-1}$. The IR evidence obtained in the absence or presence of additional NO shows a transient new absorption at 1695 cm^{-1} which can be assigned to an N–O stretching vibration in I_1 . The decay of the IR band upon further NO bubbling indicates that I_1 is also unstable under these conditions. Complementary evidence is provided by recent reports on the coordination of NO to ferrous nitrosyl porphyrins (P) giving *trans*-Fe(P)(NO)₂ in low-temperature solutions (P = TPP, *meso*-tetraphenylporphinato, and TmTP, *meso*-tetra-*m*-tolylporphinato).³⁴ These are also EPR-silent

complexes and have been characterized by UV-vis, NMR, and IR spectroscopies, showing in the latter case an intense band at 1695 cm^{-1} and a much weaker band at 1777 cm^{-1} . The presently reported labeling results for I_1 lead to similar conclusions about its structural identity. The shift of 40 cm^{-1} is close to that observed for *trans*-Fe(P)(NO)₂,³⁵ consistent with a doubly labeled dinitrosyl species. As a result of the theoretical calculations, a *trans*-syn (C_{2v}) conformation has been proposed for Fe(TPP)(NO)₂^{35,36} and similar geometries have been calculated for hypothetical model analogues, such as $[\text{M}(\text{NH}_3)_4(\text{NO})_2]^{2+}$ (M = Fe, Ru).³⁵ We anticipate, here, some preliminary results from DFT calculations for the proposed $[\text{Fe}(\text{CN})_4(\text{NO})_2]^{2-}$ complex which also reproduce the *trans*-syn geometry and provide fairly consistent ν_{NO} values at 1725 and (weaker) 1826 cm^{-1} for the singlet dinitrosyl species.

The decomposition of I_1 occurs through a disproportionation process, as described by eq 6.



The stoichiometry found for NP/ N_2O (2:1 mole ratio) agrees with reactions 6 and 7. The ability to detect I_1 is consistent with the values of the rate constants k_{first} and k_{second} in Table 1 and also agrees with the UV-vis and IR evidence on the time scale of the detection of the intermediate. Particularly revealing is the systematic appearance of rate-constant values around 10^{-5} s^{-1} , obtained through different types of measurements, either for the decay of $[\text{Fe}(\text{CN})_4\text{NO}]^{2-}$ or for the formation of the products, including the rate of formation of N_2O . By considering the concentration of NO under steady-state conditions for reactions 4–6, we find $k_{\text{first}} = 2k_4$. The mechanistic picture is consistent with NO dissociation controlling the nitrosyl transfer to other acceptors, as previously observed with intermolecular NO transfer from Mn- to Fe-tropocoronand complexes.³⁷

In reaction 6, we propose an intramolecular electron transfer in I_1 leading to bound NO^+ and NO^-/HNO , followed by the release of the latter species. Fast coupling of HNO generates N_2O , eq 7, as described elsewhere.³⁸ More evidence on this decomposition mode for I_1 is given by the complementary results obtained when unlabeled NO reacts with $[\text{Fe}(\text{CN})_4^{15}\text{NO}]^{2-}$. The intermediate shift (ca. 20 cm^{-1}) corresponds to the presence of coupled oscillators of ^{14}NO and ^{15}NO in I_1 . Most importantly, not only labeled NP but also unlabeled NP is formed as a product. This occurs because there is a probability for each nitrosyl to be oxidized or reduced in the intramolecular process.

The stoichiometric results strongly support the intramolecular reaction path in the absence of excess NO. This

(32) An excess of cyanide was used in the work reported in ref 13 providing for the near exclusion of $[\text{Fe}(\text{CN})_4(\text{NO})]^{2-}$ as well as for the fast scavenging of the $[\text{Fe}(\text{CN})_5\text{H}_2\text{O}]^{3-}$ ion in the ensuing reaction 2. This allowed us to obtain $k_{-\text{NO}} = 1.6 \times 10^{-5} \text{ s}^{-1}$ at 25 °C from the $[\text{Fe}(\text{CN})_5\text{NO}]^{3-}$ ion in a clean manner.

(33) Olabe, J. A.; Zerga, H. O. *Inorg. Chem.* **1983**, *22*, 4156–4158.

(34) Lorkovic, I.; Ford, P. C. *J. Am. Chem. Soc.* **2000**, *122*, 6516–6517.

(35) Patterson, J. C.; Lorkovic, I. M.; Ford, P. C. *Inorg. Chem.* **2003**, *42*, 4902–4908.

(36) Conradie, J.; Wondimagegn, T.; Ghosh, A. *J. Am. Chem. Soc.* **2003**, *125*, 4968–4969.

(37) Franz, K. J.; Lippard, S. J. *Inorg. Chem.* **2000**, *39*, 3722–3723.

(38) Shafirovich, V.; Lyman, S. V. *Proc. Natl. Acad. Sci. U.S.A.* **2002**, *99*, 7340–7345.

means that NO^+ and NO^- must be formed as bound species in the first event. Direct evidence is provided for NO^+ but not for NO^- (or HNO). This is understandable because of its high lability. However, HNO has been well established in the literature as a precursor to N_2O . The labeling experiments reinforce the identity of I_1 as well as its decomposition mode.

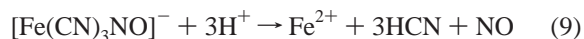
The process described by eqs 4–7 appears to be the first reported example of dinitrosyl formation and decomposition starting from a mononitrosyl complex without external NO assistance. It takes advantage of the trans effect of bound NO (eq 1) and thus promotes ligand interchange between cyanide and NO itself, coming from autodissociation. The intramolecular character of I_1 disproportionation (eq 6) is also in contrast with external NO-assisted processes reported in the literature. These have been observed following coordination of NO to several metal centers (Mn, Re, Fe, Ru, Os, Ni, Cu) forming, successively, mono- and dinitrosyls, which decompose in the presence of more NO to give N_2O and nitrite. A different picture appears for each of the metals considered with some ambiguity remaining on the detailed mechanistic issues.¹⁵

In contrast with previous studies regarding disproportionation,³⁹ the above-mentioned Fe(P)(NO)_2 complex remains stable for hours even at ambient temperature when compared with the Ru analogue which readily leads to bound nitrite and N_2O .⁴⁰ Remarkably, the disproportionation process is observed with Fe(TPP)(NO) only if trace amounts of NO_2 are present.⁴¹ The contrast with our reactive $[\text{Fe(CN)}_4(\text{NO})_2]^{2-}$ complex may be related to the low value for the $\text{Fe(NO}^+)/\text{Fe(NO)}$ redox couple (-0.37 V vs SCE)⁷ which makes NP a very stable product when one of the NO ligands in I_1 induces an electron transfer to the opposite NO. On the other hand, a potential of 0.74 V has been reported for the formal Fe(III)/Fe(II) couple in Fe(TPP)NO ⁴² suggesting a high comparative stability of the Fe(II)NO fragment in the dinitrosyl species.

Finally, the experiments at pH 4–5 show some common as well as distinctive features with respect to those at the higher pHs. The formation of NP (50% yield) and N_2O suggest a disproportionation route similar to that previously described. There is a remarkable increase in the decomposition of $[\text{Fe(CN)}_4\text{NO}]^{2-}$ at pH 4 (2 orders of magnitude faster, cf. Table 2). As the decomposition is also enhanced by some metal ions, we propose that this is because of the labilization of cyanide. Our results show that the addition of cyanide suppresses the pH effect. Then, equilibrium 8 can be proposed

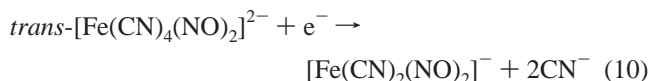


Some evidence for the existence of $[\text{Fe(CN)}_3(\text{NO})]^-$ has been reported.⁷ This species decomposes according to eq 9, releasing cyanide and NO to the reaction medium under pH conditions where HCN is stabilized. A conversion of Fe(II) from low-spin to high-spin is probably operative at a given stage of the decomposition process thus favoring the faster release of cyanide and NO.



A novel issue introduced by the results at pH 4–5 is the appearance of intermediate I_2 . Remembering that the EPR-silent intermediate in Figure 6 (pH 5) is the previously described I_1 , we propose that the latter either may evolve through disproportionation, as already discussed, or may also react leading to the new four-coordinate dinitrosyl species, I_2 , as is evident from the final spectrum in Figure 6a coincident with the one obtained after reacting $[\text{Fe(CN)}_4\text{NO}]^{2-}$ with NO (Figure 6b, see Results). The IR results in Figure 8 provide additional evidence for the identity of I_2 , $[\text{Fe(CN)}_2(\text{NO})_2]^-$. The NO-stretching frequencies are remarkably close to those reported for $[\text{Fe(CO)}_2(\text{NO})_2]^+$,^{31c} viz. 1810 and 1767 cm^{-1} . The IR absorptions of these dinitrosyl complexes have been shown to be significantly influenced by the binding properties of the spectator ligands, L.³¹

The conversion of I_1 to I_2 can be formally described by eq 10



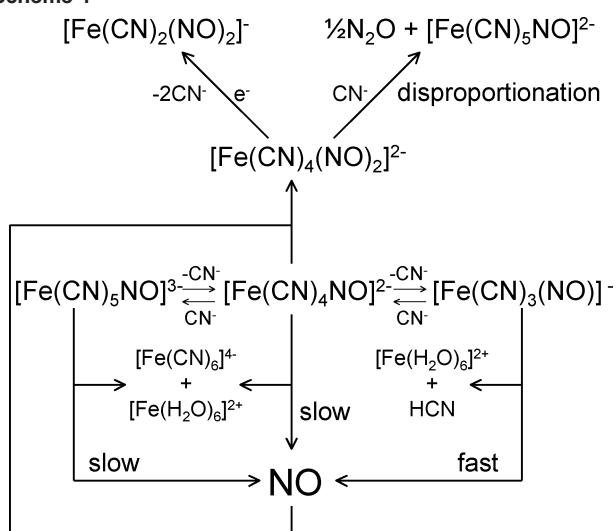
The initial five-coordinate reactant, $[\text{Fe(CN)}_4\text{NO}]^{2-}$ (eq 4), is an $\{\text{FeNO}\}^7$ species, and its configuration has been described as a d^7 Fe(I) with a NO^+ ligand.^{11c} Addition of NO forms intermediate I_1 , a six-coordinate $\{\text{Fe(NO)}_2\}^8$ species (eq 5), for which a distribution of d^6 Fe(II) with two NO radicals as ligands may be envisioned. In reaction 10, I_1 reacts to form a product, I_2 , which is a four-coordinate species, $\{\text{Fe(NO)}_2\}^9$ ($S = 1/2$). The description of the electronic structure for the latter species is still a matter of discussion, either d^7 Fe(I) with two NO ligands^{31f} or d^9 Fe(-I) with two NO^+ ligands.^{31j} Reaction 10 requires a one-electron reduction which may be accomplished by free NO or by aqueous ferrous ions.

Conclusions

We present in Scheme 1 an overall description of the decomposition processes that occur after the one-electron reduction of NP. The kinetic results show that the dissociation rates of NO from the penta- or tetracyanonitrosyl ions are very slow, $k_{-\text{NO}} \approx 10^{-5} \text{ s}^{-1}$, even at pH 7. Evidently, these rates can hardly account for the rapid vasodilatory action displayed by NP upon injection in biological fluids. In contrast to literature reports,¹² we show that even the well-established fast release of the *trans*-cyano ligand from $[\text{Fe(CN)}_5\text{NO}]^{3-}$ is not associated with a significant labiliza-

- (39) (a) Lin, R.; Farmer, P. J. *J. Am. Chem. Soc.* **2001**, *123*, 1143–1150. (b) Yoshimura, T. *Inorg. Chim. Acta* **1984**, *83*, 17–21. (c) Settin, M. F.; Fanning, J. C. *Inorg. Chem.* **1988**, *27*, 1431–1435. (d) Ellison, M. K.; Schulz, C. E.; Scheidt, W. R. *Inorg. Chem.* **1999**, *38*, 100–108.
- (40) Lorkovic, I. M.; Ford, P. C. *Inorg. Chem.* **1999**, *38*, 1467–1473.
- (41) (a) Lorkovic, I. M.; Ford, P. C. *Inorg. Chem.* **2000**, *39*, 632–633. (b) Lim, M. D.; Lorkovic, I. M.; Wedeking, K.; Zanella, A. W.; Works, C. F.; Massick, S. M.; Ford, P. C. *J. Am. Chem. Soc.* **2002**, *124*, 9737–9743. (c) Kurtikyan, T. S.; Martirosyan, G. G.; Lorkovic, I. M.; Ford, P. C. *J. Am. Chem. Soc.* **2002**, *124*, 10124–10129.
- (42) Olson, L. W.; Schaeper, D.; Lancon, D.; Kadish, K. M. *J. Am. Chem. Soc.* **1982**, *104*, 2042–2044.

Scheme 1



tion of NO from the metal. A substantial decrease in pH, down to at least 4, or any other factor favoring the release of more cyano ligands from $[\text{Fe}(\text{CN})_4\text{NO}]^{2-}$ is required for the liberation of NO to the medium. Coordinated cyanide is a strong electron donor because of its free lone pair on the nitrogen.⁴³ Thus, even in the absence of a decrease in pH, local situations may provide for protein attachment to cyanides, as recently proposed,^{1,44} favoring a complete decomposition of the complex. This can also be aided by the ubiquitous presence of appropriate metal ions, such as copper, as demonstrated in this work.

The fate of the released NO originates from two types of dinitrosyl intermediates. They have been selectively characterized under different pH conditions. The EPR-silent *trans*-dinitrosyl complex $[\text{Fe}(\text{CN})_4(\text{NO})_2]^{2-}$, described as $\{\text{Fe}(\text{NO})_2\}$,⁸ is formed through addition of NO to $[\text{Fe}(\text{CN})_4\text{NO}]^{2-}$ and shows remarkable similarities with a recently described $\text{Fe}(\text{TPP})(\text{NO})_2$ complex, also formed by coordination of NO to $\text{Fe}(\text{TPP})\text{NO}$. Although the latter complex is stable, the *trans*- $[\text{Fe}(\text{CN})_4(\text{NO})_2]^{2-}$ complex is the precursor for disproportionation, regenerating NP and evolving N_2O in a 2:1 mole ratio. This reaction is probably not significant in biological media relevant to sGC activation because NO binds to sGC faster (ca. $10^8 \text{ M}^{-1} \text{ s}^{-1}$)⁸ than it binds to $[\text{Fe}(\text{CN})_4\text{NO}]^{2-}$ (ca. $10^4 \text{ M}^{-1} \text{ s}^{-1}$, this work).

Under conditions of spontaneous decomposition (no external NO), the intermediate I_1 was characterized through UV-vis, IR, and EPR spectroscopy. We performed some preliminary DFT calculations on I_1 in which the *trans*-syn geometry was obtained, as for related dinitrosyl complexes. Kinetic evidence (first order in the complex and in NO) also points to the formation of I_1 .

Formation of N_2O and NP were *quantitatively* detected through mass spectrometry and chemical analysis, respec-

tively. IR supports the formation of N_2O , conclusively, which correlates with the decomposition of I_1 . The stoichiometry for the formation of these products was determined carefully and found to be $[\text{NP}]/[\text{N}_2\text{O}] = 2:1$. This is in agreement with our proposed mechanism for the decomposition of I_1 .

At the lower pHs, the EPR-silent $[\text{Fe}(\text{CN})_4(\text{NO})_2]^{2-}$ intermediate becomes a precursor of another dinitrosyl species, $[\text{Fe}(\text{CN})_2(\text{NO})_2]^-$. We propose it to be a new member of the well-characterized series of paramagnetic distorted tetrahedral complexes, $\{\text{Fe}(\text{L})_2(\text{NO})_2\}$, with different L ligands, described as $\{\text{Fe}(\text{NO})_2\}$.⁹ They are known to be reversible labile NO carriers effecting the *trans*-nitrosylation processes.¹⁶ EPR signals assignable to these dinitrosyl complexes have been found in tissue of ascite tumors of mice upon injection with NP.^{31f} Some of them, viz., L = thiolates and imidazole, activate sGC to promote vasodilation.^{31h,45}

The detection of dinitrosyl compounds as precursors for disproportionation is of fundamental concern in metal-NO coordination chemistry, most relevant to the enzymatic behavior of nitrite- and NO-reductases.^{15,46} A very recent report on the NO inhibition of FUR (a non-heme ferric uptake regulator protein) describes the characterization of two dinitrosyl species with proposed $\{\text{Fe}(\text{NO})_2\}$ ⁸ and $\{\text{Fe}(\text{NO})_2\}$ ⁹ structures affording spectroscopic properties surprisingly similar to those reported here for intermediates I_1 and I_2 .⁴⁷ Dinitrosyl formation, beyond the mononitrosyl coordination stage, has been described as being responsible for the conformational changes associated with NO inhibition of FUR. Some controversy still exists on related processes that seem to be present during the activation of sGC leading to smooth muscle relaxation.⁸

Acknowledgment. The authors gratefully acknowledge financial support from the Deutsche Forschungsgemeinschaft and the Volkswagenstiftung as well as from the University of Buenos Aires and the Argentine Government Agencies ANPCYT and CONICET. We specially thank Prof. Valentín T. Amorebieta for the mass-spectrometric experiments. J.A.O. and F.R. are a member of the scientific staff and a fellow of CONICET, respectively.

Supporting Information Available: Additional figures: SI1, spectral residues of the SPECFIT analysis; SI2-4, IR spectral changes recorded at pH 7; SI5, IR spectral changes recorded at pH 4; SI6, UV-vis spectral changes recorded at pH 5.2 with a SPECFIT output of the kinetic traces; and SI7, chronoamperograms for the release of NO from reduced NP in the presence of different metal ions. This material is available free of charge via the Internet at <http://pubs.acs.org>.

IC050070C

(43) Baraldo, L. M.; Forlano, P.; Parise, A. R.; Slep, L. D.; Olabe, J. A. *Coord. Chem. Rev.* **2001**, *219-221*, 881-921.

(44) Kowaluk, E. A.; Seth, P.; Fung, H. L. *J. Pharmacol. Exp. Ther.* **1992**, *262*, 916-922.

(45) Vanin, A. F.; Stukan, R. A.; Mabuchkina, E. B. *Biochim. Biophys. Acta* **1996**, *1295*, 5.

(46) (a) Wasser, I. M.; de Vries, S.; Moëgne-Loccoz, P.; Schröder, I.; Karlin, K. D. *Chem. Rev.* **2002**, *102*, 1201-1234. (b) Averill, B. A. *Chem. Rev.* **1996**, *96*, 2951-2964.

(47) D'Autrèaux, B.; Horner, O.; Oddou, J. L.; Jeandey, C.; Gambarelli, S.; Berthomieu, C.; Latour, J. M.; Michaud-Soret, I. *J. Am. Chem. Soc.* **2004**, *126*, 6005-6016.